

# Exploring Halo Substructure with Giant Stars: The Velocity Dispersion Profiles of the Ursa Minor and Draco Dwarf Spheroidals At Large Angular Separations

Ricardo R. Muñoz<sup>1</sup>, Peter M. Frinchaboy<sup>1</sup>, Steven R. Majewski<sup>1</sup>, Jeffrey R. Kuhn<sup>2</sup>, Mei-Yin Chou<sup>1</sup>, Christopher Palma<sup>3</sup>, Sangmo Tony Sohn<sup>1,4</sup>, Richard J. Patterson<sup>1</sup> & Michael H. Siegel<sup>1,5</sup>

## ABSTRACT

We analyze velocity dispersion profiles for the Draco and Ursa Minor (UMi) dwarf spheroidal (dSph) galaxies based on published and new Keck HIRES spectra for stars in the outer UMi field. Washington+*DDO*51 filter photometric catalogs provide additional leverage on membership of individual stars, and beyond 0.5 King limiting radii ( $r_{\text{lim}}$ ) identify *bona fide* dSph members up to 4.5 times more efficiently than simple color-magnitude diagram selections. Previously reported “cold populations” at  $r_{\text{lim}}$  are not obvious in the data and appear only with particular binning; more or less constant and platykurtic dispersion profiles are characteristic of these dSphs to large radii. We report discovery of UMi stars to at least  $2.7r_{\text{lim}}$  (i.e., 210' or 4 kpc). Even with conservative assumptions, a UMi mass of  $M > 4.9 \times 10^8 M_{\odot}$  is required to bind these stars, implying an unlikely global mass-to-light ratio of  $M/L > 900 (M/L)_{\odot}$ . We conclude that we have found stars tidally stripped from UMi.

*Subject headings:* galaxies: individual (Ursa Minor dwarf spheroidal, Draco dwarf spheroidal) – galaxies: kinematics and dynamics – Local Group

---

<sup>1</sup>Dept. of Astronomy, University of Virginia, Charlottesville, VA 22903-0818 (rrm8f, pmf8b, srm4n, mc6ss, rjp0i@virginia.edu)

<sup>2</sup>Institute for Astronomy, University of Hawaii, Honolulu HI 96822 (kuhn@ifh.hawaii.edu)

<sup>3</sup>Dept. of Astronomy & Astrophysics, Penn State, University Park, PA 16802 (cpalma@astro.psu.edu)

<sup>4</sup>Korea Astronomy and Space Science Institute, 61-1 Hwaam-Dong, Yuseong-Gu, Daejeon 305-348 Korea (tonysohn@kasi.re.kr)

<sup>5</sup>University of Texas – McDonald Observatory Austin, TX 78712 (siegel@astro.as.utexas.edu)

## 1. Introduction

Dwarf spheroidal (dSph) galaxies are thought to be strongly dark matter (DM) dominated, with global mass-to-light ( $[M/L]_{\text{tot}}$ ) ratios ranging from a few to hundreds in solar units. Spectroscopic databases are now available for some dSphs to their King limiting radii,  $r_{\text{lim}}$  (Kleyna et al. 2004; Wilkinson et al. 2004, hereafter W04), and beyond (Tolstoy et al. 2004; Westfall et al. 2005; R. Muñoz et al., in preparation, hereafter M05), enabling investigation of the dSph kinematics and inferred mass distribution to large radii. Yet, very low stellar densities, still formidably challenge efficient spectroscopic study of dSphs at large angular separations. The photometric filtering techniques that are the basis of this series of papers successfully overcome this problem and can substantially increase the radial extent of dSph dynamical surveys.

Derived radial velocity (RV) dispersion ( $\sigma_v$ ) profiles for dSphs tend to remain rather flat to well past the core radius. Kleyna et al. (2002) attempted to fit the flat Draco (Dra) dSph profile using two-parameter spherical models (Wilkinson et al. 2002) that yield increasing  $M/L$  with radius and a net  $(M/L)_{\text{tot}}$  of  $440 \pm 240$ . Lokas (2002), applying a constant anisotropy parameter model to the  $\sigma_v$  profiles of the Fornax and Dra dSphs, derived  $\sim 10^9 M_\odot$  masses for these two systems. Cosmology-dependent studies (Stoehr et al. 2002; Hayashi et al. 2003) based on  $\Lambda$ CDM models interpret the flat  $\sigma_v$  profiles as consistent with massive DM halos surrounding luminous cores. This interpretation helps alleviate the “missing satellites” problem (Kauffmann et al. 1993; Klypin et al. 1999; Moore et al. 1999) endemic to these cosmologies. MW tidal effects on dSphs have also been considered (e.g., Hodge & Michie 1969; Kuhn & Miller 1989; Kuhn 1993; Kroupa 1997; Gómez-Flechoso et al. 1999; Fleck & Kuhn 2003; M05) with predictions of potentially significant unbound stellar populations producing flat/rising dSph  $\sigma_v$  profiles.

W04 and Kleyna et al. (2004) recently reported flat or slightly rising  $\sigma_v$  profiles that suddenly decline near the  $r_{\text{lim}}$  of the Dra, Ursa Minor (UMi) and Sextans dSphs. Such widely separated cold populations in dSphs are of interest because they have been interpreted as signs of *mild* tidal disruption, but more importantly, because they severely mitigate against the idea of extended, heated populations around dSphs (W04). How far dSphs really extend as well as the bound versus unbound nature of putative “extratidal” components remains unanswered. Spectroscopic observation of dSph-associated stars beyond  $r_{\text{lim}}$  is thus important to confirm the reality of the extended populations and to ascertain their dynamical state.

In this *Letter* the W04 RVs up to  $r_{\text{lim}}$  for Dra and UMi are combined with new RVs for UMi stars to several  $r_{\text{lim}}$  to reassess the  $\sigma_v$  profiles of these dSphs. Washington+DDO51 filter photometry aids our discrimination of dSph giant star members. We show that: (1)

UMi members exist well past  $r_{\text{lim}}$  (§3). (2) The  $\sigma_v$ 's of Dra and UMi remain more or less constant to past  $r_{\text{lim}}$  (§5). (3) A cold population at  $r_{\text{lim}}$  for one of the dSphs is found only under certain binning schemes, and furthermore, depends on how one defines outliers (§5). (4) The Washington+*DDO*51 method is at least 5 times more efficient at finding *bona fide* dSph members than color magnitude diagram (CMD)-selection schemes (§4).

## 2. Photometric and Spectroscopic Data

Previous contributions in this series (Majewski et al. 2000a; Majewski et al. 2000b; Palma et al. 2003, hereafter P03; Westfall et al. 2005) show that Washington+*DDO*51 photometry effectively identifies rare dSph giant star members against the high Milky Way foreground in the low density wings of dSphs (see §4). We use a similar methodology here, where giant star candidates are first selected within the two-color diagram (2CD) boundary shown in Fig. 1. The UMi photometry is from P03 supplemented with similar Mosaic camera data along the northeast UMi major axis taken with the Mayall 4-meter telescope on UT 2002 May 4-6. The Dra photometry was obtained with the MiniMosaic (MiniMo) camera and WIYN telescope on UT 2004 March 12-13 and 2005 April 16-19. MiniMo's field of view is not optimal for large area photometric surveys; these data were taken as a backup project when the instrument for our primary observing program failed. As a consequence we only partially surveyed Dra, covering a total area of  $\sim 0.84 \text{ deg}^2$ . Median photometric errors for this dataset are  $(\sigma_M, \sigma_{T_2}, \sigma_{DDO51}) = (0.014, 0.014, 0.018)$  at  $M = 21.0$

We have been unable to obtain spectroscopic follow-up of Dra giant candidates identified with our photometry. However, M. Wilkinson graciously provided the W04 RV database for 416 and 266 observed stars in the directions of the Dra and UMi dSphs, respectively. Typical RV errors for these data are 2.4 (Dra) and 2.9  $\text{km s}^{-1}$  (UMi). We cross-identify by celestial coordinates 254 UMi field stars (95%) but only 212 Dra field stars (51%) between the W04 and our databases.

To these data we add Keck HIRES (Vogt et al. 1994) spectra for 52 UMi field stars obtained UT 2002 May 21-22 and UT 2004 May 12-13 (data available from authors). We deliberately targeted UMi giant candidates at large radii. The spectra were reduced with standard IRAF echelle reduction methodology with RVs determined using the `fxcor` package on the Mg triplet ( $5130 - 5210 \text{ \AA}$ ) order. Our quoted RV errors are determined as in Vogt et al. (1995) with a median of 4.3  $\text{km s}^{-1}$ , calibrated by 19 multiple measures of six different UMi stars. For nine stars in common with Armandroff, Olszewski, & Pryor (1995) we obtain a mean RV difference of 0.3  $\text{km s}^{-1}$  with dispersion of only 2.9  $\text{km s}^{-1}$ . The union of our data with that of W04 yields 309 unique RVs for the UMi field.

### 3. Revisiting dSph Membership

The Washington+*DDO*51 database can be used not only to select dSph giant star candidates *before* spectroscopy (as done here for UMi) but for after-the-fact assessment of likely membership of stars in existing RV catalogues. Figure 1 shows our CMD and 2CD for UMi and Dra. Filled/open circles designate RV stars more/less likely to be giants based on positions in the 2CD (with “giants” adopted as stars bounded by the thin line). A few stars just outside our giant selection criteria that have an RV consistent with that of the dSph have been considered giants as well. The “likely giant stars” tend to lie closer to the red/asymptotic giant branches of the dSphs than the “less likely giants” (Fig. 1).

Figure 2 shows RVs for all stars versus elliptical radius,  $r_e$ , normalized to  $r_{\text{lim}} = 77.9$  for UMi (P03) and 40.1 for Dra (Odenkirchen et al. 2001). An “elliptical radius” corresponds to the semi-major radius of the ellipse centered on the dSph that intersects the position of the star and has the measured ellipticity of the dSph (0.54 for UMi and 0.29 for Dra; from above references). We adopt elliptical rather than circular radii to follow the distribution of stars, although a dSph’s gravitational potential and tidal boundary do not necessarily mimic its observed shape (we revisit circular radii in §5).

The W04  $3\sigma$  rejection criterion to discriminate likely dSph members (dashed lines in Fig. 2) corresponds to  $\pm 39 \text{ km s}^{-1}$  around  $\langle RV \rangle = -290.8 \text{ km s}^{-1}$  for Dra and  $\pm 36 \text{ km s}^{-1}$  around  $\langle RV \rangle = -245.2 \text{ km s}^{-1}$  for UMi. By these criteria (Fig. 2) only six of our photometric Dra giant candidates lie outside this velocity range, proving the reliability of our photometric discrimination technique. Among stars classified as giants by our photometric technique, two (solid squares in Fig. 2) lie just outside the RV range at  $-246.1 \pm 4.6 \text{ km s}^{-1}$  and  $-332.03 \pm 4.8 \text{ km s}^{-1}$  (uncertainties within  $1\sigma$  of the “Dra member” RV limit). While for  $\sim 200$  Dra members one expects only  $\sim 0.5$  outliers at  $> 3\sigma$  for a *Gaussian* distribution, the kurtosis excesses ( $\gamma_2$ ) of *both* the Dra and UMi RV distributions flatten from near Gaussian ( $\gamma_2 = 0$ ) to  $\gamma_2 = -0.8$  and  $-0.9$ , respectively, at  $r_e > 0.4r_{\text{lim}}$ , so that more *apparent* “outliers” might be expected. Based on these two arguments and the “giant star” colors of these two stars we consider them to be very likely Dra members.

In UMi, a larger number of giant candidates than in Dra live clearly outside the RV criteria (Fig. 2). Because even the faintest stars with RVs have quite small photometric uncertainties (P03), it is not likely that these “false positives” are due to photometric error, but rather represent field halo giants or metal-poor dwarf stars with weak Mgb+MgH absorption. Among the “non-UMi” giant candidates there appears to be RV clumpiness, with 9/9/7 stars having  $\sigma_v = 9.2 \pm 2.3 / 9.6 \pm 2.6 / 16.6 \pm 4.6 \text{ km s}^{-1}$  around  $\langle RV \rangle = 6.4 / -54.8 / -163.8 \text{ km s}^{-1}$ , respectively. These RV clumps of giant candidates have  $\sigma_v$ ’s of order those observed in UMi and Dra, as well as in the Sagittarius (Sgr) tidal tails (Majewski et al. 2004) and are rem-

iniscient of foreground halo substructure discovered in our similar survey of Carina (M05); our giant star identification method may be finding *other* halo substructure in the UMi field. Nevertheless, the majority of stars we photometrically classify as giants do lie inside the W04 “UMi” RV range (see §4). A remaining photometric giant candidate (*triangle*) lies just outside the UMi RV limits but well inside the giant region in the 2CD *and* along the RGB locus for UMi; we strongly suspect this star is a UMi member and include it in our  $\sigma_v$  analysis (§5). In the end, 182 UMi and 210 Dra stars are included in our  $\sigma_v$  profiles (§5).

#### 4. Photometric efficiency

Particularly at large angular radii, the sky density of dSph stars with brightnesses amenable to current spectroscopic capability (i.e., red giants) is swamped by foreground stars. To improve overall efficiency of target selection, various groups (e.g., W04) select dSph targets by position on/near the dSph’s giant branch in the CMD. This typically decreases foreground contamination by an order of magnitude but “false positive” sources still well outnumber dSph stars outside  $r_{\text{lim}}$  (Majewski et al. 2005; Westfall et al. 2005). However, our Washington+*DDO*51 photometric technique improves sample reliability by an additional order of magnitude over, for example, the W04 CMD selection.

Over all angular separations (to  $r_e = 7.7r_{\text{lim}}$  in the case of UMi) our technique yields a dSph member identification efficiency of 87% for UMi and 97% for Dra. Our “false positive” identifications all lie beyond  $0.5r_{\text{lim}}$  (we ignore the possibility that their RV clumping is due to wrapped UMi tidal debris arms, as observed in the Sgr system; Majewski et al. 2003). W04’s overall success rate for their CMD-selected candidates, to only  $r_e \sim 0.8r_{\text{lim}}$  for UMi and  $r_e \sim 1.8r_{\text{lim}}$  for Dra, is 62% and 50%, respectively. Considering targets with  $r_e/r_{\text{lim}} > 0.5$ , the W04 efficiency drops to 38% (28/73) and 19% (45/239) respectively, whereas our selection method at similar radii still nets an overall efficiency of 77% (23/30) and 85% (23/27) for UMi and Dra. This 2 to 4.5 times greater member selection efficiency optimizes the exploration of low density dSphs galaxies with valuable 6 to 10-m class telescope time.

#### 5. Velocity Dispersion Profiles and Interpretation

Our  $\sigma_v$  profiles are computed using equal sample-size binning, but similar results are found with equal, linear bin sizes (though some bins are poorly populated in this scheme). The method of Armandroff & Da Costa (1986) is used to calculate  $\sigma_v$ , because a Maximum Likelihood method like that used by W04 assumes a Gaussian velocity distribution at all

radii, which is not observed for either dSph, and is also not expected in a disrupted system (M05). To assess the influence of bin size and geometry Figure 3 shows the UMi dispersion profile versus elliptical (panel a) and circular radii (panel b) with 17, 12 and 7 members per bin (and the outermost bins accumulating any odd, extra star). As expected, profile variability is less pronounced as the number of stars per bin increases. The general UMi trend is an initial decline in  $\sigma_v$  followed by a gentle rise and then a slightly decreasing profile. The sudden decline to a “cold point” reported by W04 appears only in the highest resolution binning that is most susceptible to statistical fluctuations. While larger samples of stars in the outer regions of dSphs would be helpful, UMi seems to share the trend of more or less flat dispersion profiles observed in the outskirts of other dSphs (Mateo 1997, Westfall et al. 2005, M05).

The Dra profiles (Fig. 4) use 21, 16 and 8 stars per bin, with solid circles for the 208 star samples. Open symbols show the outer profiles when the stars marked as squares in Figure 2 are included. Except for a single bin in the lower profile of panel (b), the same general  $\sigma_v$  behavior is seen at large radii as in UMi: a flat (or maybe slowly decreasing) profile (depending on the binning) is observed past  $r_{\text{lim}}$ . In fact, a non-binning test, like the “one-by-one” test used by Kleyana et al. (2004) for Sextans, does not show a cold population in the outermost dispersion points for either dSph. Moreover, a  $\chi^2$  fit of the  $\sigma_v$  distribution to a constant value for both UMi and Dra shows that there is no evidence that the outermost stars have a  $\sigma_v$  that is statistically different from those of stars at smaller projected radii.

Tidal disruption can create an unbound stellar population near a dSph. This seems to be a natural explanation for producing *both* the observed extended stellar distributions *and* flat/slowly declining velocity dispersion profiles at large radii in dSphs (Kuhn & Miller 1989; Kroupa 1997; Mayer et al. 2002, Fleck & Kuhn 2003; M05). While the flat  $\sigma_v$  profiles observed in UMi and Dra have also been modeled by an *ad hoc* extended DM halo (Kleyana et al. 2002), two additional pieces of evidence support a tidal disruption scenario. First, the observed platykurtic velocity distributions at large radii in both UMi and Dra more closely match the flattened RV distributions of unbound dSph stars at large radii in detailed N-body tidal disruption simulations (e.g. M05).

Second, our new Keck RVs have verified the most widely separated member stars for any dSph other than the tidally disrupting Sgr galaxy. Our most separated UMi-field star having a UMi RV is at a linear distance of 238' (4.8 kpc) and near the minor axis; this star’s elliptical radius of  $r_e = 6.6r_{\text{lim}}$  implies a major axis radius of 10.4 kpc if the UMi ellipticity is maintained at all radii. Assuming a spherical potential for UMi, the required mass to keep this star bound to the dSph is  $M > 3M_{\text{MW}}(r/R_{\text{GC}})^3$ , or  $7.6 \times 10^8 M_\odot$  for a Milky Way mass within the UMi distance ( $R_{\text{GC}} = 69$  kpc) of  $M_{\text{MW}} = 7.6 \times 10^{11} M_\odot$  (Burkert 1997); this

translates to  $(M/L)_{\text{tot}} > 1,400 (M/L)_{\odot}$  when we adopt  $L = 5.4 \times 10^5 L_{\odot}$  (P03). However, if the tidal boundary of UMi is more elongated, a larger  $M/L$  is implied; at the limit where the tidal boundary is elongated according to its central ellipticity, this star, were it placed at its corresponding major axis radius (i.e.,  $r = r_e$  or 10.4 kpc), implies an astounding UMi  $(M/L)_{\text{tot}} > 14,400 (M/L)_{\odot}$  for UMi.

It might be argued that the latter star is a field halo interloper, since its RV is only  $\sim 60 \text{ km s}^{-1}$  (to the retrograde side) of that expected for a non-rotating halo (assuming a  $232 \text{ km s}^{-1}$  solar rotation about the Galactic center) and within the  $\sigma_v$  of a hot MW halo ( $\sim 100 \text{ km s}^{-1}$ ; e.g., Sirko et al. 2004). Higher  $S/N$  spectroscopy to test this star’s chemical properties would be useful. However, under the above MW dynamics, the second most separated “RV member” — at  $210'$  (4 kpc), or  $r_e = 2.7r_{\text{lim}}$  along the UMi major axis — is retrograde by  $\sim 105 \text{ km s}^{-1}$ . A UMi-bound star at this projected radius implies a UMi mass  $> 4.9 \times 10^8 M_{\odot}$  or  $(M/L)_{\text{tot}} > 900 (M/L)_{\odot}$ .

One could use a Milky Way model, like the Besancon model ([http : //bison.obs – besancon.fr/modele/](http://bison.obs-besancon.fr/modele/)) to estimate the expected Milky Way background; this model predicts  $\sim 3.2$  MW halo giants in the range of RV, color and magnitude of the present  $9.7 \text{ deg}^2$  UMi survey area outside  $r_{\text{lim}}$ , under the assumption that we have observed *all* possible targets in the field, whereas we have only observed 37% (implying about 1 interloper in our  $> r_{\text{lim}}$  RV sample). However, the Besancon model uses smooth population density laws to describe *mean* densities and does not account for second order substructure perturbations. In the case that our color-color-magnitude-RV sampling of parameter space happens to be dominated by a substructure “void”, the Besancon model background should be an overestimate. Were our sampling instead *overpopulated* by substructure, the model would underestimate the background. But the presence of the substructure should be obvious by coherence in our parameter space, while, for there to be interlopers within our UMi sample, these stars would have to both lie at roughly the UMi distance (to share position in the CMD and 2CD) and have about the UMi RV — a situation we consider improbable. Moreover, the Besancon model in fact *overpredicts* by  $2.3\times$  the number of Milky Way stars we see *outside* the UMi RV-member range; accounting for this factor, in the limit of a smooth halo, implies only 0.5 Milky Way contaminants within the UMi RV sample. In the end, we regard as unlikely that *both* of the outermost UMi RV members are contaminants.

If either of these outer dSph stars are bound, UMi has the largest  $M/L$  of any galaxy by yet *another* order of magnitude *or two* than previously suggested. The corresponding physical dimensions of UMi would rival the King profile extent of the Sgr density distribution, of which a significant fraction, however, has been shown must be *unbound* (Majewski et al. 2003). From the extreme physical dimensions implied it is difficult to avoid the conclusion

that true extratidal stars have now been identified for the UMi system — results consistent with suggestions of tidal disruption of this dSph by photometric analyses as early as that of Hodge (1964) and more recently by Martínez-Delgado et al. (2001), P03, and Gómez-Flechoso & Martínez-Delgado (2003). The existence of shared photometric and RV trends between UMi and Dra to at least  $r_{\text{lim}}$  points to a possible tidal disruption scenario for Dra as well (e.g., Smith, Kuhn, & Hawley 1997).

We gratefully acknowledge support by NSF grant AST-0307851, NASA/JPL contract 1228235, the David and Lucile Packard Foundation, Frank Levinson through the Celerity Foundation, the Virginia Space Grant Consortium, and the IfA/UH. We thank the referee, N. Wyn Evans for helpful suggestions to improve the paper.

## REFERENCES

- Armandroff, T. E., & Da Costa, G. S. 1986, *AJ*, 92, 777
- Armandroff, T. E., Olszewski, E. W., & Pryor, C. 1995, *AJ*, 110, 2131
- Burkert, A. 1997, *ApJ*, 474, L99
- Fleck, J. & Kuhn, J. R. 2003, *ApJ*, 592, 147
- Gómez-Flechoso, M. A., Fux, R., & Martinet, L. 1999, *A&A*, 347, 77
- Gómez-Flechoso, M. Á. & Martínez-Delgado, D. 2003, *ApJ*, 586, L123
- Hayashi, E., Navarro, J. F., Taylor, J. E., Stadel, J., & Quinn, T. 2003, *ApJ*, 584, 541
- Hodge, W. P. 1964, *AJ*, 69, 438
- Hodge, P. W. & R. W. Michie 1969, *AJ*, 74, 587
- Kauffmann, G., White, S. D. M., & Guiderdoni, B. 1993, *MNRAS*, 261, 201
- Kleyna, J. T., Wilkinson, M. I., Evans, N. W., Gilmore, G., & Frayn, C. 2002, *MNRAS*, 330, 792
- Kleyna, J. T., Wilkinson, M. I., Evans, N. W., & Gilmore, G. 2004, *MNRAS*, 354, L66
- Klypin, A., Kravtsov, A. V., Valenzuela, O., & Prada, F. 1999, *ApJ*, 522, 82
- Kroupa, P. 1997, *New Astronomy*, 2, 139



- Kuhn, J. R. & Miller, R. H. 1989, *ApJ*, 341, 41
- Kuhn, J. R. 1993, *ApJ*, 409, L13
- Lokas, E. L., 2002, *MNRAS*, 333, 697
- Majewski, S. R., Ostheimer, J. C., Kunkel, W. E., & Patterson, R. J. 2000a, *AJ*, 120, 2550
- Majewski, S. R., Ostheimer, J. C., Patterson, R. J., Kunkel, W. E., Johnston, K. V., & Geisler, D. 2000b, *AJ*, 119, 760
- Majewski, S. R., Skrutskie, M. F., Weinberg, M. D., & Ostheimer, J. C. 2003, *ApJ*, 599, 1082
- Majewski, S. R., et al. 2004, *AJ*, 128, 245
- Majewski, S. R., et al. 2005, *AJ*, in press (astro-ph/0503627)
- Martínez-Delgado, D., Alonso-García, J., Aparicio, A., & Gómez-Flechoso, M. A. 2001, *ApJ*, 549, L63
- Mateo, M. 1997, *ASP Conf. Ser.*, 116, 259
- Mayer, L., Moore, B., Quinn, T., Governato, F. & Stadel, J. 2002, *MNRAS*, 336, 119
- Moore, B., Ghigna, S., Governato, F., Lake, G., Quinn, T., Stadel, J., & Tozzi, P. 1999, *ApJ*, 524, L19
- Odenkirchen, M. et al. 2001, *AJ*, 122, 2538
- Palma, C., Majewski, S. R., Siegel, M. H., Patterson, R. J., Ostheimer, J. C., & Link, R. 2003, *AJ*, 125, 1352 (P03)
- Sirko, E., et al. 2004, *AJ*, 127, 914
- Smith, H. A., Kuhn, & Hawley, S. L. 1997, *ASP Conf. Ser.*, 127, 163
- Stoehr, F., White, S. D. M., Tormen, G., & Springel, V., 2002, *MNRAS*, 335, L84
- Tolstoy et al., 2004, *ApJ*, 617, L119
- Vogt, S. S., et al. 1994, *Proc. SPIE*, 2198, 362
- Vogt, S. S., Mateo, M., Olszewski, E. W., & Keane, M. J. 1995, *AJ*, 109, 151

Westfall, K. B., Majewski, S.R., Ostheimer, J. C., Frinchaboy, P. M., Kunkel, W.E., Patterson, R. J., Link, R. 2005, AJ, in press

Wilkinson, M. I., Kleyana, J. T., Evans, N. W., & Gilmore, G. F. 2002, ApJ, 330, 778

Wilkinson, M. I., Kleyana, J. T., Evans, N. W., Gilmore, G. F., Irwin, M. J., & Grebel, E. K. 2004, ApJ, 611, L21 (W04)

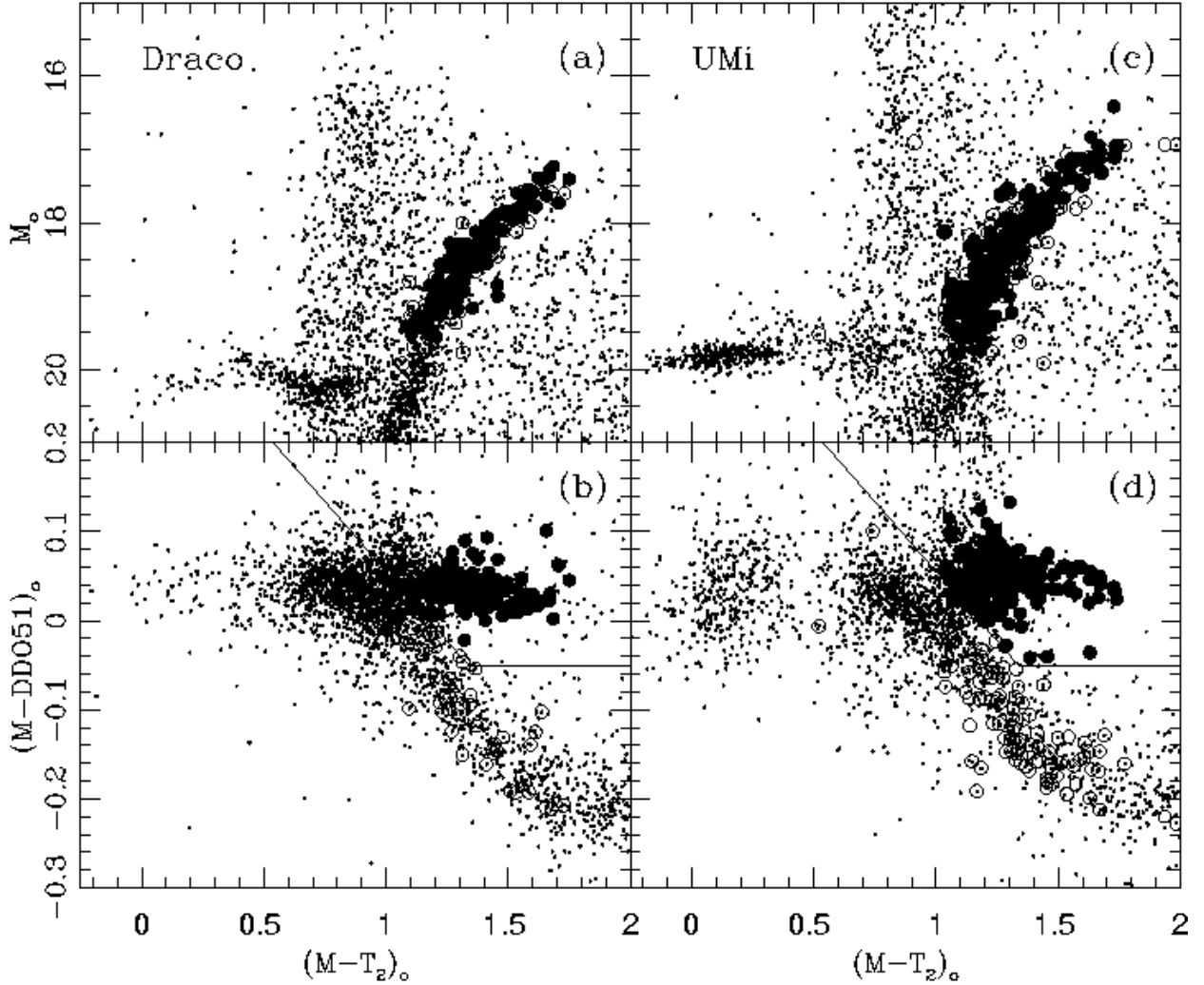


Fig. 1.— (a) Color-magnitude diagram (CMD) for the Dra dSph photometric catalog. Solid/open circles show stars with available RV data selected/not selected photometrically to be Dra giants based on panel (b). (b)  $(M - T_2, M - DDO51)_o$  diagram for the same data as panel (a). (c) and (d): CMD and 2CD for the UMi dSph from P03. For clarity, only stars within one  $r_{\text{lim}}$  have been plotted. Symbols in (c) and (d) have similar meaning as for panels (a) and (b) but for the UMi field.

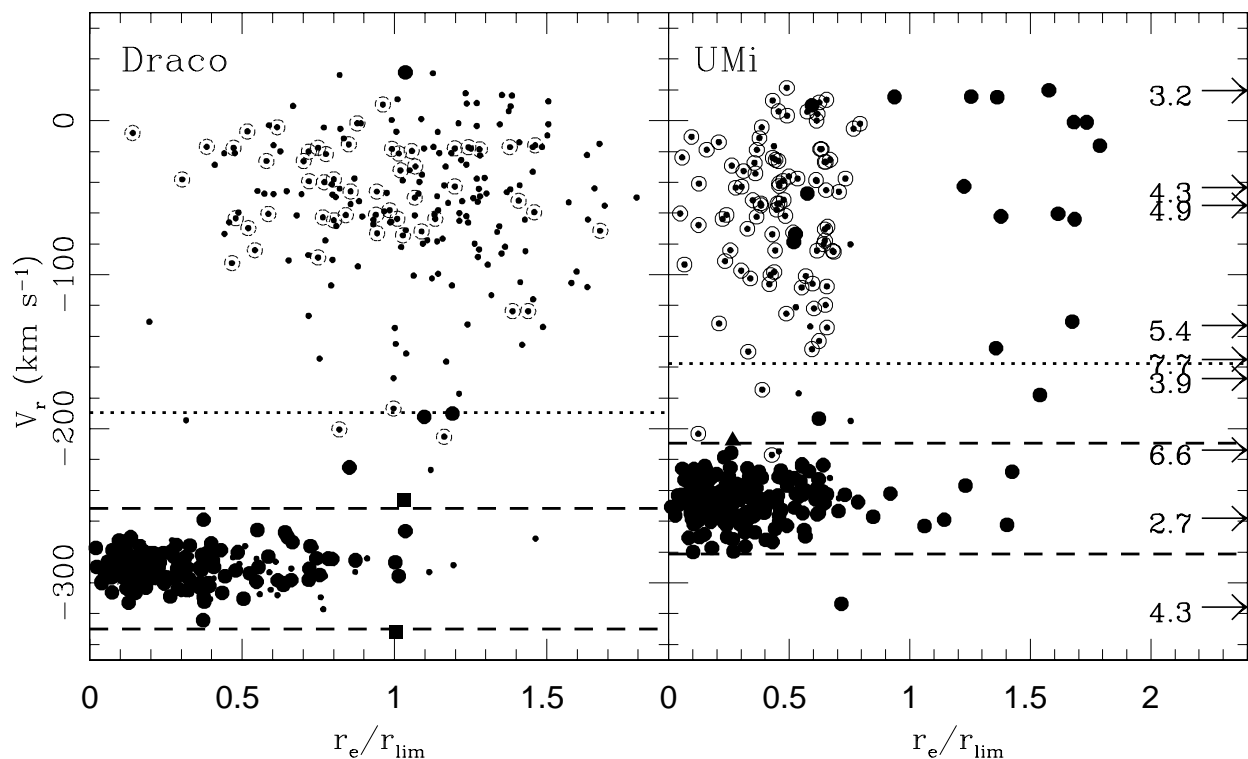


Fig. 2.— RV versus elliptical radius (normalized to  $r_{\text{lim}}$ ) for the Dra (a) and UMi (b) dSphs. Symbols are as in Fig. 1. Dashed lines delineate the  $3\sigma$  RV range adopted as dSph membership criteria by W04. Arrows indicate the RVs of stars outside the plotted area (normalized radii indicated for these stars next to their arrows). Dotted lines show RV expected for zero Galactic rotation velocity, assuming a  $232 \text{ km s}^{-1}$  solar rotation velocity about the MW.

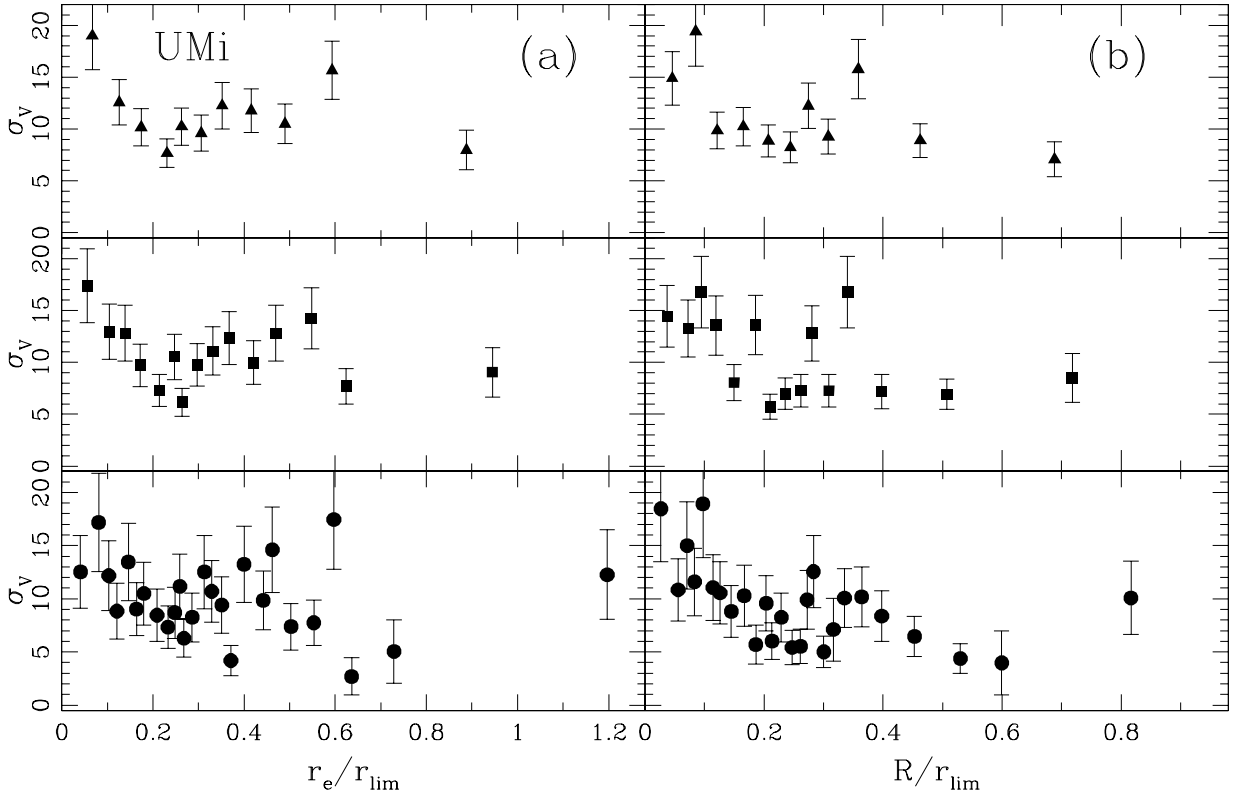


Fig. 3.— RV dispersion profiles for the UMi dSph. The panels use (top to bottom) 17, 12 and 7 stars per bin. Solid symbols show  $\sigma_v$ 's calculated from the 182 star sample. Panels show profiles versus (a) elliptical and (b) circular radii.

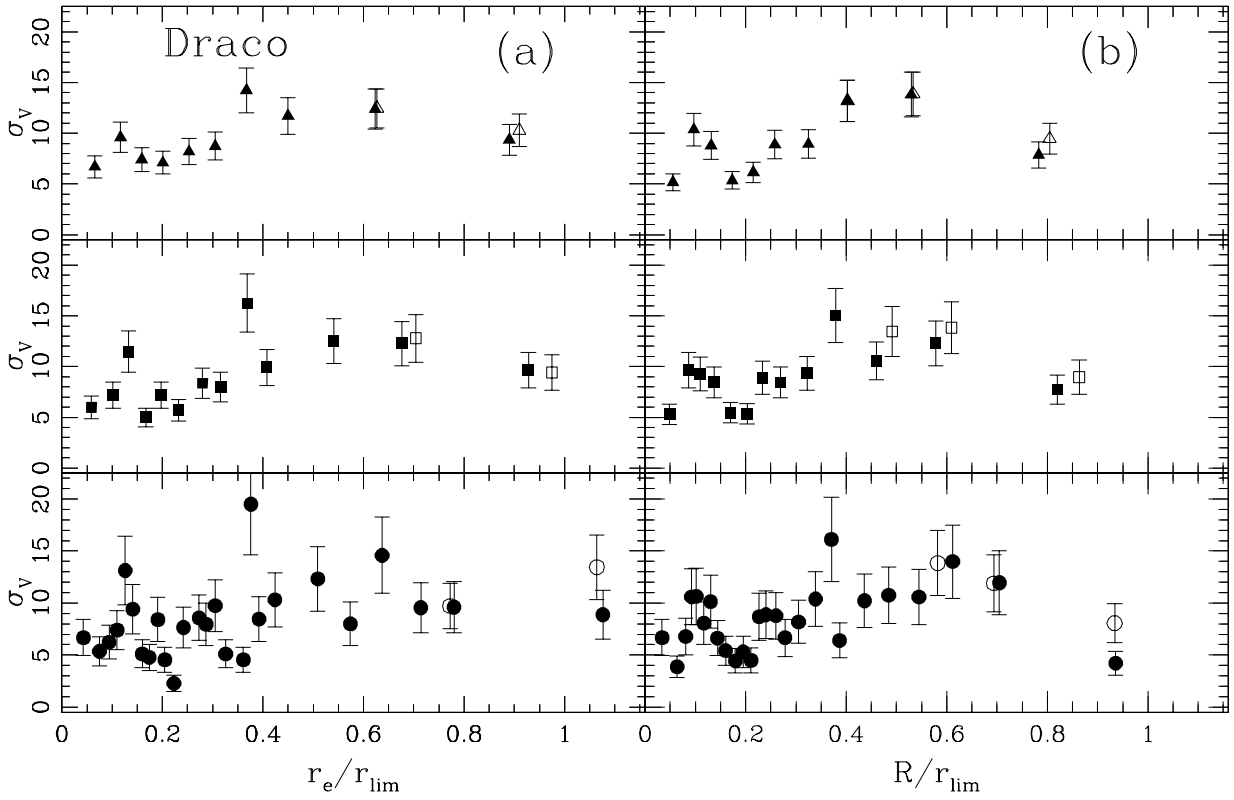


Fig. 4.— Same as Fig. 3 for the Dra dSph. From upper to lower panel, 21, 16 and 8 stars are used per bin. Open symbols show the profile when the stars shown by squares in Fig. 2 are included.